Journal of Engineering and Applied Research (JEAR)

National University of Skills

Winter & Spring 2025, Vol. 2, No. 1, p. 74-100

Journal Homepage: https://jear.tvu.ac.ir

:10.48301/jear.2025.495732.1059

A new method in investigating the robust stability of linear controllers designed for the automatic voltage regulation (AVR) system of synchronous generators

Mohammad Reza Modabbernia [1*], Kaveh Hariri Asli [2], Seyed yaser Fakhrmoosavi [3]

[1,3] Department of Electrical Engineering, Technical and Vocational University (TVU), Tehran, Iran

[2] Department of Mechanical Engineering, Technical and Vocational University (TVU), Tehran, Iran

ARTICLE INFO

Article Type:
Original Research

Received: 01.18.2025
Revised: 02.08.2025
Accepted: 04.12.2025

Keyword:
Automatic voltage regulation
resistive control
P-Δ-K
synchronous generator

***Corresponding Author:**
Mohammad Reza Modabbernia
Email: *mmodabernia@tvu.ac.ir*

ABSTRACT

In this work, a method is presented to analyze the robust stability of the optional linear controller provided for the automatic terminal voltage adjustment (AVR) of the synchronous generator connected to the infinite bus system (SMIB). The robust control approach and μ theorem shape the structure of the presented manner. It could be used to check the robust stability of all linear controllers designed for the AVR system. In this regard, first, the closed-loop model of the AVR system is introduced, and the range of system parameter changes is expressed in the form of real values. Then, the general P-K structure related to the robust control theory of this system is presented without considering the functional weight functions. In this structure, the blocks P and Delta are determined exactly, and K is the transfer function or state-space equations of the desired controller that the analyzer seeks to specify its robust stability. This controller could be designed in any manner. A flowchart is provided for the above process. Finally, by using the introduced P-K model and flowchart, we will investigate the robust instability of three PID controllers optimized with metaheuristic algorithms that have been proposed in the references for the AVR system.

E-ISSN: 3060-6357

Introduction

Due to the complex behavior of the power system, such as the nonlinearity of the system characteristics, the load changes of the variable working points, and the high inductance value of the generator field coils, it is not easy to achieve a fast and stable response from the voltage regulator [1]. Therefore, it is important to improve the performance, robustness, and speed of the AVR through a controller to ensure the reliable response of the closed-loop system to the time changes of the terminal voltage. In this regard, various control strategies have been proposed for the AVR system.

Because of the simple structure and easy use of proportional-integral-derivative (PID) controllers in the industry [2], these controllers are widely used to create a good performance for the AVR system. In recent years, with the growth of meta-heuristic optimization algorithms, it has been seen that a large number of proportional-integral (PI) and PID controllers, as well as controllers derived from them, such as fractional-order PID (FOPID) and fuzzy logic PID is proposed for AVR system based on these optimization algorithms. Designing a decentralized PI controller and adjusting its parameters using the Bacteria Foraging (BF) algorithm and Bacteria Foraging Particle Swarm Optimization (BFPSO) have been discussed and reviewed in reference [3]. PID controllers by particle swarm optimization (PSO) methods [4], artificial bee colony algorithm [5], [6], jumping frog algorithm (SFL) [7], particle swarm optimization algorithm simplified [8], Taguchi genetic algorithm method [9], local uni-exponential sampling algorithm [10], teaching-learning optimization algorithm (TLBO) [11] and colonial competition algorithm (ICA) [12] have been made. A combination of genetic algorithm (GA) and fuzzy logic method have been used by Duraj and Selvabala for the optimized parameters of PID controller in AVR system [13]. An optimization technique of irregular ant swarm has been reported by Teng and his colleagues for the PID controller of the AVR system [14]. In [15], the particle swarm algorithm (PSO) was used to optimize the linear fractional PID controller (FOPID). An adaptive controller with direct fractional order base model (Direct-FOMRAC) for AVR is presented, whose parameters are optimized using adaptive rules defined by fractional order differential equations [16]. Zhang and his colleagues have proposed an improved artificial bee colony algorithm (CNC-ABC) to adjust FOPID controller parameters [17]. In [18], various criteria of AVR have been structured into system software and then checked with a multi-objective optimization (MOO) algorithm. The optimized FOPID controller with Colonial Competition Algorithm (ICA) is designed for the AVR system in reference [19].

Mokherji and Koshal have focused on the optimal setting of the PID controller of the AVR system using the craziness-based particle swarm optimization

algorithm (CRPSO) and the binary-coded genetic algorithm [20]. The performance of PID, F-PID, and GA-F-PID controllers have been tested to improve the energy efficiency of a Jahdi and Ardhali dynamic energy system [21]. In [22], the fuzzy discrete PID controller is applied to the single-machine model connected to the infinite bus (SMIB). A fuzzy logic controller based on limit value sets for modeling uncertainties caused by system uncertainties has been introduced by Panda et al. [23]. PSO algorithm has been used to adjust four parameters of the PID controller with second order derivative (PID2) by Sahib [24]. The Cuckoo algorithm has been used to adjust the parameters of the fractional linear PID controller of the AVR system [25]. In [26], the Equilibrium Optimizer (EO) algorithm has been used to determine the optimal values of PID parameters for the AVR system. Moreover, a novel objective function for PID parameter determination is proposed. Based on the equations used in our paper, Modabbernia et al. designed an AVR robust controller based on the H infinity approach [27]. The significant use of robust control and theory to improve the performance of power systems in the last two decades has been reported by Fan [28]. In [29], a robust multivariable controller based on infinite soft minimization of the closed-loop structure of the generator excitation system is presented. Bohamida et al. have evaluated a controller to improve the transient behavior and the steady-state condition of a synchronous machine connected to a bus with a constant voltage through the transmission line [30]. μ-Synthesis has been used to design a 10th-order robust controller for wind turbines [31].

Articles related to the design of industrial controllers for automatic synchronous generator voltage regulation (AVR) are mostly in line with the optimization of PID controllers in a specific working point. These articles tried to show the stability of the closed-loop system by simulating the closed-loop structure at different operating points of the AVR system after optimizing the controller coefficients. This manner has two essential problems. First, in the process of controller designing, the operating point of the system is generally considered to be in low gains, and the system becomes unstable simply by increasing the gains several times. Second, simulating several different operating points is not an acceptable method for showing the controller's robustness. Acceptance is not intended to prove the robust stability of the controller. The current article seeks to introduce a comprehensive and complete solution to this problem by presenting the P-Δ_u-K model of the AVR system and defining a flowchart to calculate its robustness with robust control μ-theorem.

This article has been organized as follows: i) The control structure of the single-zone power system connected to the infinite bus is introduced. ii) The AVR system of a synchronous generator connected to the infinite bus is modeled, and its parameters are introduced in practice. iii) The basic principles of robust control based on μ-theory are briefly reviewed for analysis of the closed-loop systems with real-parametric uncertainties. iv). The P-Δ_u -K model of the AVR system of a synchronous generator connected to an infinite bus is presented, followed by a flowchart for analyzing the robust stability of linear controllers designed based on this P-Δ_u -K model. v). The robust or non-robust stability of three linear controllers designed in the references has been analyzed, based on the presented method.

2- The control structure of the single zone power system connected to the infinite bus

An interconnected power system can be considered as a set of single-zone power systems connected to an infinite bus (SMIB) that are connected to the national grid through a transmission line. The beating heart of SMIB is a synchronous generator, which must maintain terminal voltage stability, frequency stability, rotor angle stability, and synchronism with the power system in different operating conditions. Figure 1 shows the classical control structure of an SMIB to maintain the mentioned stability conditions.

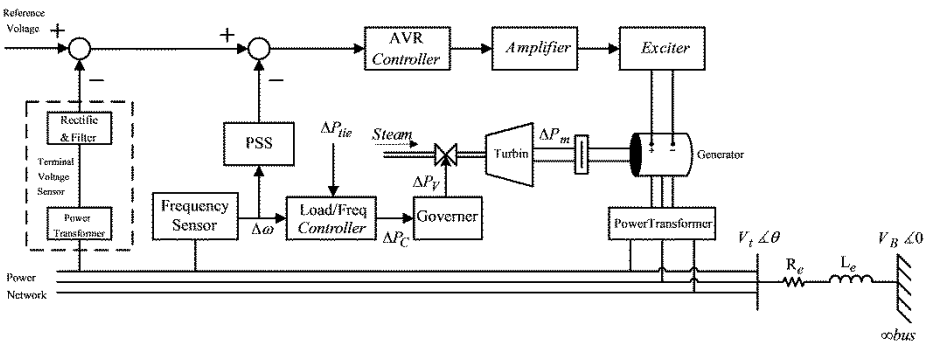

Figure 1. Classical control structure of a single zone power system connected to an infinite bus (SMIB)

In the structure of Figure 1, the changes of low active power depend on the changes in the rotor angle and frequency. On the other hand, the reactive power produced by the generator depends on the size of the terminal voltage and consequently the excitation current of the field coil. Because the time constant of the excitation system is much lower than the time constant of the primary

stimulus, therefore, its transient fluctuations are quickly weakened and have little effect on the load frequency control (LFC) dynamics. As a result, the mutual effects of the LFC and AVR loops are ignored, and the analysis and design of these two systems have been done independently [30]. However, the basic problem of these two control structures lies in their ability to remove and destroy transient mode oscillations (LFO) [32, 33]. To solve this problem, another control loop called the Power System Stabilizer (PSS) is used in the classic SMIB control structure, which, upon receiving the frequency error signal, provides an additional input signal for the AVR controller to dampen the LFO oscillations as quickly as possible. Figure 2 shows the block diagram of this classic structure for voltage and frequency control of the SMIB system. Based on Figure 2, three separate control structures 1- automatic voltage adjustment or AVR, 2- power system stabilizer or PSS, and 3- load frequency control or LFC can be considered to adjust the voltage and frequency of the synchronous generator connected to the infinite bus defined.

3- Linear model of automatic voltage regulation system of synchronous generator (AVR)

By removing the parts related to the frequency output, i.e. PSS and LFC in Figure 2, the automatic voltage regulation system of the synchronous generator will remain. Figure 3 shows the block diagram of the AVR system in the Simulink environment. In AVR modeling to stabilize the generator voltage, the amplifier, exciter, voltage sensor, and synchronous generator are modeled with a first-order transformation function, whose gain and time constant change in a certain range as shown in Table 1. By Assuming a) the stability of the gain value and the time constant of the voltage sensor and b) the definition of the new gain parameter of the forward path, we can define the uncertain parameters of the AVR system in the form of equations 1 to 6 and in the form of structured uncertainties. This definition is done by considering the maximum and minimum values of the gain of the forward path and the time constant of other transformation functions, as well as the nominal value and relative size of changes for this gain and time constant.

$$\begin{cases} K_F = K_{F(nom)}\left(1+\delta_{KF}\, P_{KF}\right) \\ T_a = T_{A(nom)}\left(1+\delta_{TA}\, P_{TA}\right) \\ T_e = T_{E(nom)}\left(1+\delta_{TE}\, P_{TE}\right) \\ T_g = T_{G(nom)}\left(1+\delta_{TG}\, P_{TG}\right) \end{cases} \quad (1)$$

Where $T_{A(nom)}$, $T_{E(nom)}$, $T_{G(nom)}$, and $K_{F(nom)}$ are the nominal values of the parameters and P_{TA}, P_{TE}, P_{TG}, and P_{KF} are the relative size of the changes of these parameters and are defined as follows:

$$\begin{cases} K_{F(nom)} = \dfrac{K_{F(\max)} + K_{F(\min)}}{2} \\ P_{KF} = \dfrac{K_{F(\max)} - K_{F(\min)}}{K_{F(\max)} + K_{F(\min)}} \end{cases} \quad (2)$$

$$\begin{cases} T_{A(nom)} = \dfrac{T_{a(\max)} + T_{a(\min)}}{2} \\ P_{TA} = \dfrac{T_{a(\max)} - T_{a(\min)}}{T_{a(\max)} + T_{a(\min)}} \end{cases} \quad (3)$$

$$\begin{cases} T_{E(nom)} = \dfrac{T_{e(\max)} + T_{e(\min)}}{2} \\ P_{TE} = \dfrac{T_{e(\max)} - T_{e(\min)}}{T_{e(\max)} + T_{e(\min)}} \end{cases} \quad (4)$$

$$\begin{cases} T_{G(nom)} = \dfrac{T_{g(\max)} + T_{g(\min)}}{2} \\ P_{TG} = \dfrac{T_{g(\max)} - T_{g(\min)}}{T_{g(\max)} + T_{g(\min)}} \end{cases} \quad (5)$$

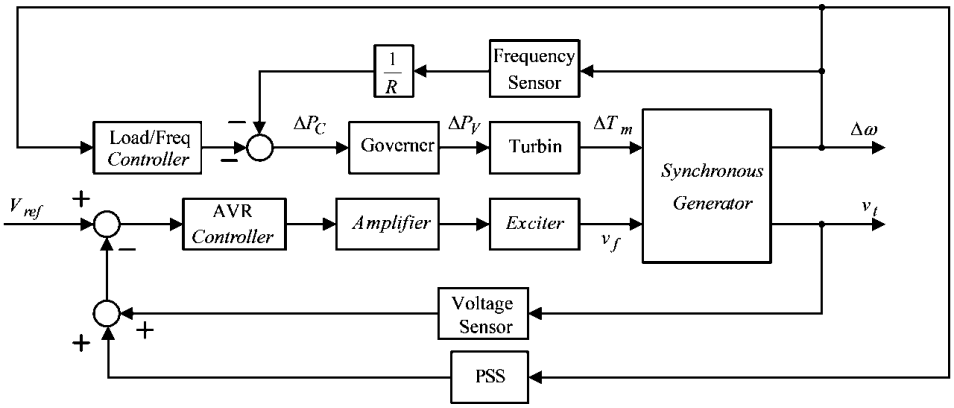

Figure 2. The classical combination of the frequency and voltage regulation of the single generator connected to infinite bus (SMIB)

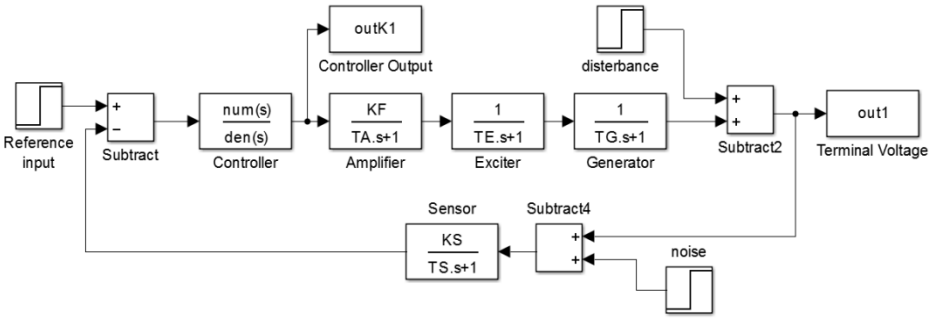

Figure 3. The classical combination of the frequency and voltage regulation of the single generator connected to infinite bus (SMIB)

Table 1. AVR system parameters and their change ranges

parameters	changes range of time constant	changes range of gain	Nominal value and relative size of time constant	nominal value and relative size of gain changes	Conversion function
changes of components	$0.02\text{s} \le T_a \le 0.1\text{s}$ $T_{a(\max)} = 0.1\text{s}$ $T_{a(\min)} = 0.02\text{s}$	$10 \le K_a \le 40$ $K_{a(\max)} = 40$ $K_{a(\min)} = 10$	$\begin{cases} T_{a(nom)} = 0.06 \\ P_{Ta} = \frac{2}{3} \cong 0.666 \end{cases}$	$K_a = 1$	$G_A = \frac{K_a}{T_a s + 1}$
Amplifier	$0.4\text{s} \le T_e \le 1\text{s}$ $T_{e(\max)} = 1\text{s}$ $T_{e(\min)} = 0.4\text{s}$	$1 \le K_e \le 10$ $K_{e(\max)} = 10$ $K_{e(\min)} = 1$	$\begin{cases} T_{e(nom)} = 0.7 \\ P_{Te} = \frac{3}{7} \cong 0.428 \end{cases}$	$K_e = 1$	$G_E = \frac{K_e}{T_e s + 1}$
Exciter	$1\text{s} \le T_g \le 2\text{s}$ $T_{g(\max)} = 2\text{s}$ $T_{g(\min)} = 1\text{s}$	$0.7 \le K_g \le 1$ $K_{g(\max)} = 1$ $K_{g(\min)} = 0.7$	$\begin{cases} T_{g(nom)} = 1.5 \\ P_{Tg} = \frac{1}{3} \cong 0.333 \end{cases}$	$K_g = 1$	$G_G = \frac{K_g}{T_g s + 1}$
Generator	$0.001\text{s} \le T_s \le 0.06\text{s}$ $T_{s(\max)} = 0.06\text{s}$ $T_{s(\min)} = 0.001\text{s}$	$0.9 \le K_s \le 1.1$ $K_{s(\max)} = 1.1$ $K_{s(\min)} = 0.9$	$T_s = 0.0305$	$K_s = 1$	$G_S = \frac{K_s}{T_s s + 1}$

Sensor	-	$7 \le K \le 400$ $K_{(\max)} = 400$ $K_{(\min)} = 7$	-	$K_F = K_a K_e K_g$ $\begin{cases} K_{F(nom)} = 203.5 \\ P_{KF} = \frac{393}{407} \cong 0.966 \end{cases}$

According to Table 1, instead of considering 3 interest variables, we have defined the interest variable in the forward path, which is the product of these interests. This has reduced the number of uncertainties, but it makes us unable to include the effect of external disturbances in the input of the excitation and generator parts in the modeling process.

4- The structure needed to analyze the stability and robust performance of the controller designed based on the μ theory

Some of the parameters of the state space model or the transformation function of a system may change specifically within a known range (have changed with the structure). At the same time, all the model details may be completely inaccurate beyond a certain frequency. This inaccuracy may be caused by not modeled hysteresis, resonance, interference caused by matching, and other factors. In practice, it is always possible to show the information of uncertainties in a very precise manner like the form of Figure 4 [34]. In this structure, it has been assumed that the nominal device P has three sets of input lines and three sets of output lines.

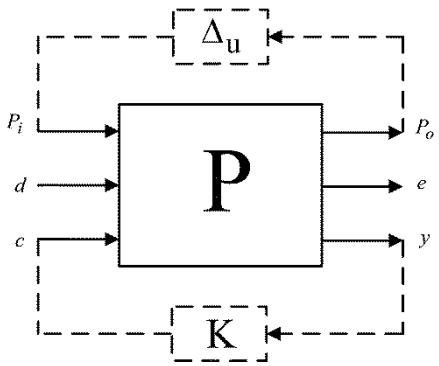

Figure 4. The standard arrangement of nominal system under control feedback in the presence of modeled uncertainties

The first set of inputs and outputs of the nominal system P, which is identified by the names Pi and Po respectively, show the outputs and inputs modeled requirements.uncertainties block of the system. The second category of inputs

includes (d) all external signals, such as disturbances, measured noise, and any uncontrollable input. The third group of inputs are control signals which are applied to the device from the output of the designed controller. The third set of outputs (c) includes all measured feedback signals. The second category (e) indicates the outputs whose behavior is intended and their size should be kept small. These error outputs (e) are not necessarily measured, although some may result from measured outputs. Block P is the nominal device plus all the weighting functions considered for modeling the unstructured uncertainties of the system. The uncertain block Δ_u includes all modeled structured and or unstructured uncertainties of the system, and the K block is the controller designed to meet the desired.

To analyze and check the stability and robust function of the proposed linear controller, it is necessary to change the P-Δ_u-K structure of Figure 4 to the standard M-Δ form of Figure 5. In this figure, $\mathrm{M} = F_L(\mathrm{P},\mathrm{K}) \in C^{m\times n}$ is the lower linear-fractional combination of the nominal device P and the designed controller that we want to measure its robust stability or performance. The block $\Delta = \begin{bmatrix} \Delta_u & 0 \\ 0 & \Delta_p \end{bmatrix}$ consists of two parts: Δ_u and The uncertain block Δ_p. The Δ_u is related to the system uncertainties. In most general situations, it can include real structured uncertainties, mixed structured uncertainties, and unstructured uncertainties. The block Δ_p with infinite norm smaller than or equal to one model the performance uncertainties associated with infinite norm minimization from outputs e to inputs d. If it is necessary to use weighting functions for this minimization. The transfer functions of these weights must be entered into the structure of the matrix M.

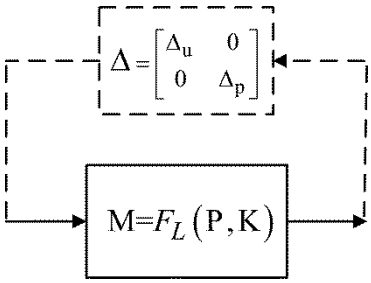

Figure 5. The standard arrangement of nominal system under feedback control in the presence of modeled uncertainties

$$\begin{cases} \mathrm{M} = F_L(\mathrm{P},\mathrm{K}) = \begin{bmatrix} \mathrm{M}_{11} & \mathrm{M}_{12} \\ \mathrm{M}_{21} & \mathrm{M}_{22} \end{bmatrix} \quad , \quad \Delta = \begin{bmatrix} \Delta_{\mathrm{u}} & 0 \\ 0 & \Delta_{\mathrm{p}} \end{bmatrix} \\ \Delta_{\mathrm{u}} = diag[\delta_1 I_{ri},...,\delta_s I_{rs},\delta_{s+1} I_{s+1},...,\delta_t I_{rt},\Delta_1,...,\Delta_W] \\ \delta_i \in R, 1 \le i \le s \;\; ; \;\; \delta_j \in C, s+1 \le j \le t \;\; ; \;\; \Delta_k \in C^{mk \times nk} \\ \Delta_{\mathrm{p}} \in C^{n_e \times n_d} \quad : \quad \left\| \Delta_{\mathrm{p}} \right\|_\infty \le 1 \end{cases} \tag{6}$$

By considering Δ, $\mu_\Delta(\mathrm{M})$ can be defined as a singular value of the transfer function M according to Δ as follows [35]:

$$\begin{cases} \mu_\Delta(\mathrm{M}) = 0 & if \quad \det[I - \mathrm{M}\Delta] \ne 0 \quad \forall \Delta \in \Delta \\ \mu_\Delta(\mathrm{M}) = \dfrac{1}{\min\{\sigma_{\max}(\Delta) : \Delta \in \mathrm{B}\Delta \;;\; \det[I - \mathrm{M}\Delta] = 0\}} & otherwise \end{cases} \tag{7}$$

$\mu_\Delta^{-1}(\mathrm{M})$, is defined as the smallest $\sigma_{\max}(\Delta)$ when Δ belongs to the set **B**Δ firstly and $\det[I - \mathrm{M}\Delta] = 0$ secondly. In other words, it can be said that μ is a function of the matrix M that depends on the structuresod $\Delta \in \mathrm{B}\Delta$ and secondly, $\mu_\Delta^{-1}(\mathrm{M})$ is the norm of the smallest Δ destabilizer that applies to the $\det[I - \mathrm{M}\Delta] = 0$ condition.

The model of Figure 5 is determined for a closed loop system with uncertainty according to the desired controller. In this model, the values of μ are associated with the components of $\mathrm{M} = F_L(\mathrm{P},\mathrm{K}) = \begin{bmatrix} \mathrm{M}_{11} & \mathrm{M}_{12} \\ \mathrm{M}_{21} & \mathrm{M}_{22} \end{bmatrix}$ and $\Delta = \begin{bmatrix} \Delta_{\mathrm{u}} & 0 \\ 0 & \Delta_{\mathrm{p}} \end{bmatrix}$. The μ value determines the level of robust stability and or the robust performance of the closed-loop system as follows: [34]

a) If $\mu_\Delta(\mathrm{M}) < 1$ then the robust operation of the closed loop system is guaranteed.

b) If $\mu_{\Delta_{\mathrm{u}}}(\mathrm{M}_{11}) < 1$ then the robust stability of the closed loop system is guaranteed.

c) If $\left\| \mathrm{M}_{22} \right\|_\infty = \mu_{\Delta_{\mathrm{p}}}(\mathrm{M}_{22}) < 1$ then the nominal performance of the closed loop system is guaranteed.

d) If M is internally stable, then the nominal stability of the closed-loop system is guaranteed.

Therefore, if the structure of Figure 4 will be calculated for the voltage regulation system of the synchronous generator (AVR) in the presence of all

uncertainties of the system, then the structure of Figure 4 can be easily converted to the form of Figure 5 for each existing designed controller. Therefore, the robust performance of this controller could be determined based on the value of ?.

5- P-Δu-K model based on μ theory for automatic voltage regulation system of synchronous generator (AVR)

The elements and parameters in the structure of the AVR system, according to Table 1, consist of two parts: the gain of (K_F) and the first-order transformation function $\left(\frac{1}{Ts+1}\right)$ with an inverse time constant $\left(\frac{1}{T}\right)$. Therefore, by introducing the P-Δ_u-K model of these two uncertainties(K_F and $\frac{1}{T}$) and including them in the combination of Figure 3, the P-Δ_u-K model of the AVR was achieved. Figures 6 and 7 show the P-Δ_u-K models of the two parts of gain and inverse of time constant, as well as the first-order transformation function.

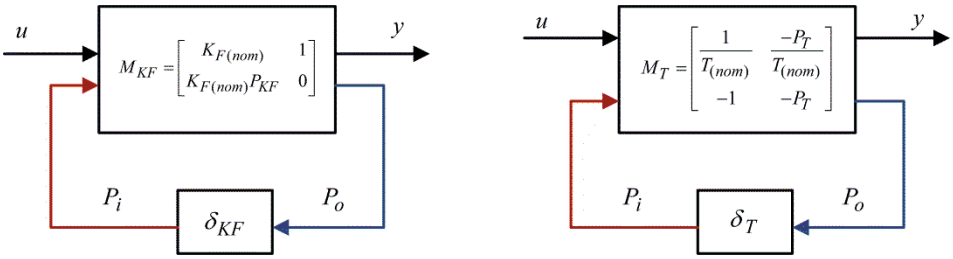

Figure 6. Standard model P-Δ_u-K gain and inverse of time constant.

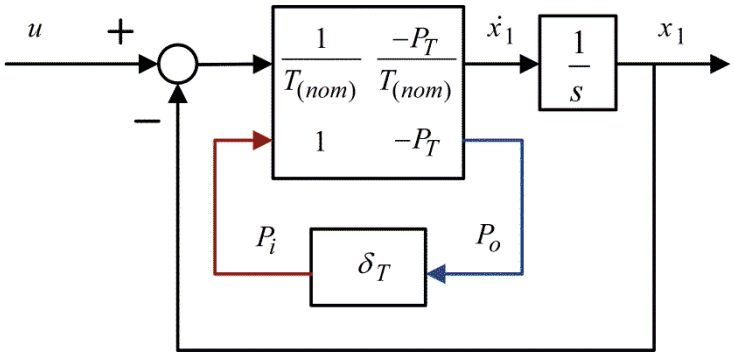

Figure 7. The standard P-Δ_u-K model of the first order transformation function with gain 1 and uncertain time constant T

Based on the models presented in Figures 6 and 7, the general structure of the synchronous generator voltage regulation system of Figure 3 can be generalized to Figure 8.

In Figure 8, the AVR system has four uncertainties, four disturbance inputs, a reference input, a disturbance input, a noise input, an input from the controller, four disturbance outputs, a terminal voltage output, and an output as a signal. The error is for the controller. Assuming that the AVR system has four modes, eight inputs and six outputs, it can be shown that the representation of the state space in Figure 8 is as follows [27]:

$$\begin{cases} \dot{x} = Ax + Bu \\ y = Cx + Du \end{cases} \qquad \text{AVR\_plant} = pck\left[A, B, C, D\right] \tag{8}$$

Where

$$A = \begin{bmatrix} \dfrac{-1}{T_{A(nom)}} & 0 & 0 & 0 \\ \dfrac{1}{T_{E(nom)}} & \dfrac{-1}{T_{E(nom)}} & 0 & 0 \\ 0 & \dfrac{1}{T_{G(nom)}} & \dfrac{-1}{T_{G(nom)}} & 0 \\ 0 & 0 & \dfrac{K_S}{T_S} & \dfrac{-1}{T_S} \end{bmatrix} \tag{9}$$

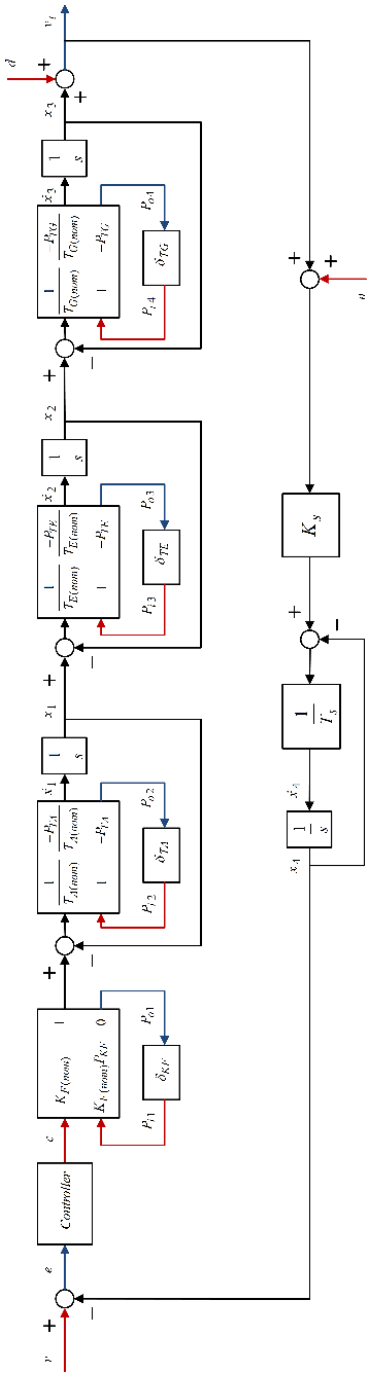

Figure 8. The general structure of the synchronous generator voltage regulation system (AVR) in the presence of real parametric uncertainties.

$$B=\begin{bmatrix}B_1 & B_2\end{bmatrix} \quad B_1=\begin{bmatrix}\frac{1}{T_{A(nom)}} & \frac{-P_{TA}}{T_{A(nom)}} & 0 & 0\\ 0 & 0 & \frac{-P_{TE}}{T_{E(nom)}} & 0\\ 0 & 0 & 0 & \frac{-P_{TG}}{T_{G(nom)}}\\ 0 & 0 & 0 & 0\end{bmatrix}$$

$$B_2=\begin{bmatrix}0 & 0 & 0 & \frac{K_{F(nom)}}{T_{A(nom)}}\\ 0 & 0 & 0 & 0\\ 0 & 0 & 0 & 0\\ 0 & \frac{K_S}{T_S} & 0 & 0\end{bmatrix} \tag{10}$$

$$C=\begin{bmatrix}C_1\\ C_2\end{bmatrix} \qquad C_1=\begin{bmatrix}0 & 0 & 0 & 0\\ -1 & 0 & 0 & 0\\ 1 & -1 & 0 & 0\\ 0 & 1 & -1 & 1\end{bmatrix} \qquad C_2=\begin{bmatrix}0 & 0 & 1 & 0\\ 0 & 0 & 0 & -1\end{bmatrix} \tag{11}$$

$$D=\begin{bmatrix}D_{11} & D_{12}\\ D_{21} & D_{22}\end{bmatrix} \qquad D_{11}=\begin{bmatrix}0 & 0 & 0 & 0\\ 1 & -P_{TA} & 0 & 0\\ 0 & 0 & -P_{TE} & 0\\ 0 & 0 & 0 & -P_{TG}\end{bmatrix}$$

$$D_{12}=\begin{bmatrix}0 & 0 & 0 & K_{F(nom)}P_{KF}\\ 0 & 0 & 0 & K_{F(nom)}\\ 0 & 0 & 0 & 0\\ 0 & 0 & 0 & 0\end{bmatrix} \qquad D_{21}=\begin{bmatrix}0 & 0 & 0 & 0\\ 0 & 0 & 0 & 0\end{bmatrix} \tag{12}$$

$$D_{22}=\begin{bmatrix}0 & 1 & 0 & 0\\ 1 & 0 & 1 & 0\end{bmatrix}$$

The P-Δ_u-K representation of the AVR system without considering the weighting functions associated with the closed-loop system operation is shown in Figure 9. In this representation, the AVR model (AVR_Plant) includes state equations of 9 to 13 and $\Delta_u = diag(\delta_{KF}, \delta_{TA}, \delta_{TE}, \delta_{TG})$ is a 4×4 structured uncertaintiy. This uncertainty is a diagonal matrix whose main diagonal elements have a specific structure and belong to the range of $[-1,1]$ real numbers. This structure can only be used to determine the robust stability of the desired

controller due to the non-inclusion of the weight functions related to the performance of the closed loop system.

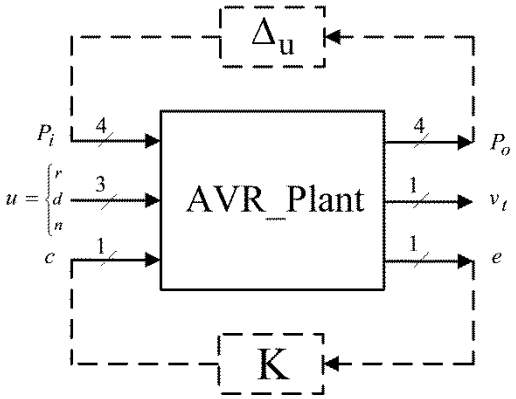

Figure 9. The standard P-Δ_u-K arrangement of the synchronous generator voltage regulation system (AVR) to determine the robust stability

Figure 10 shows the diagram of the AVR closed-loop system in the presence of an uncertainty block with a diagonal structure and desired weighting functions to meet the performance conditions. In this figure, the performance weighting function W_p is related to the terminal voltage of the generator, and limits the sensitivity function of $\left(S(s) \le W_s^{-1}(s)\right)$ so that the sensitivity of output disturbances is reduced as much as possible. This weighting function could be defined in the form of equation (14). The sensitivity function should be smaller than W_p at high frequencies (initial times) to limit the system transient time and overshoot [35, 36].

$$W_p(s) = \frac{K_{wp}\left(\frac{s}{M_p} + \omega_p\right)}{\left(s + \varepsilon_p\, \omega_p\right)} \tag{13}$$

Also, at low frequencies (finite times) in order to reduce the steady state error of the closed-loop system, the magnitude of W_p must be reduced $\left(\varepsilon_p\right)$. On the other hand, in order to limit the energy of the controller, the W_u weighting function is selected in such a way as to reduce the output size of the controller.

For this purpose, the following structure can be used for the W_u weighting function [35, 36].

$$W_u(s) = \frac{K_{wu}\left(s + \frac{\omega_u}{M_u}\right)}{\left(\varepsilon_u s + \omega_u\right)} \qquad (14)$$

Which W_u is the saturation limit of the stimulus and cannot be too large. Since ε_u there is no need for the controller to have a large response at high frequencies or early times, a small number is chosen. In addition, the bandwidth of the controller is determined by the coefficient so that the time required to reach the final value increases as it becomes larger. W_u , and are also W_{ref} W_{noise} W_{dis} ، weights that are generally defined in the form of real numbers for simplicity and specify the limit of the effect or the increase of the effect of the base inputs, disturbance inputs and noise inputs, respectively. It should be noted that frequency-dependent functions can also be considered for these weights.

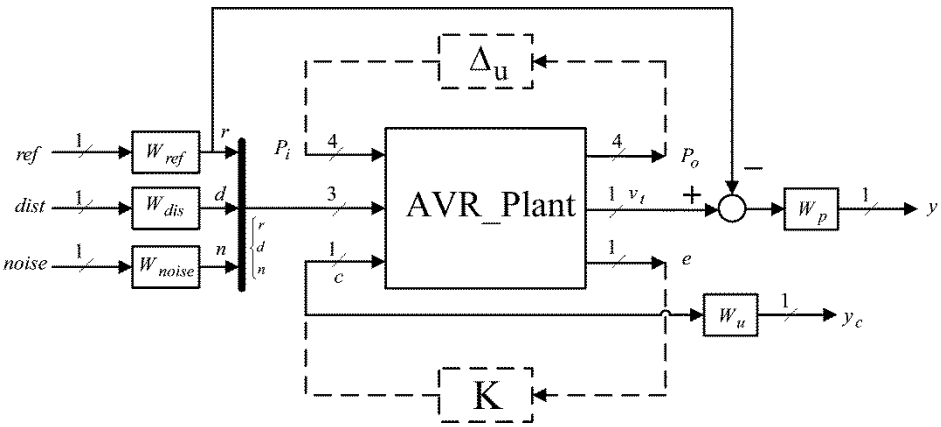

Figure 10. AVR closed loop system diagram in the presence of uncertain block with structure and weight functions

If the transfer functions or state equations of each part of Figure 10 are known, it is easy to convert the diagram of Figure 10 into the general structure of Figure 11 by using sysic, iconnect or augw commands of MATLAB software (The program written with the sysic command is given below). The difference between Figure 11 and Figure 10 is introducing of functions related to the defined functional weights into the structure of the AVR_Plant section of Figure 10 and the creation of a new AVR block. It achieves by entering the functions related to

the defined functional weights in the structure of the AVR_ Plant section of Figure 10 and creating a new AVR block. In order to analyze the rbust stability and robust performance of the desired controller, the P-Δ_u-K model should be transformed into the M-Δ structure by lower fractional transformation of the AVR block and the K controller block so that the robust stability $\left(\mu_{\Delta_u}(M_{11})<1\right)$ or robust performance $\left(\mu_{\Delta}(M)<1\right)$ could be analyzed through the μ value and determined the resistance of the closed loop system. This equation is shown in Figure 11. It should be noted that if the only goal is to determine the robust stability of the closed loop system, there is no need to model and use the weighting functions of Figure 10 and convert Figure 10 to Figure 11.In this situation, the structure of Figure 9 could be used directly.

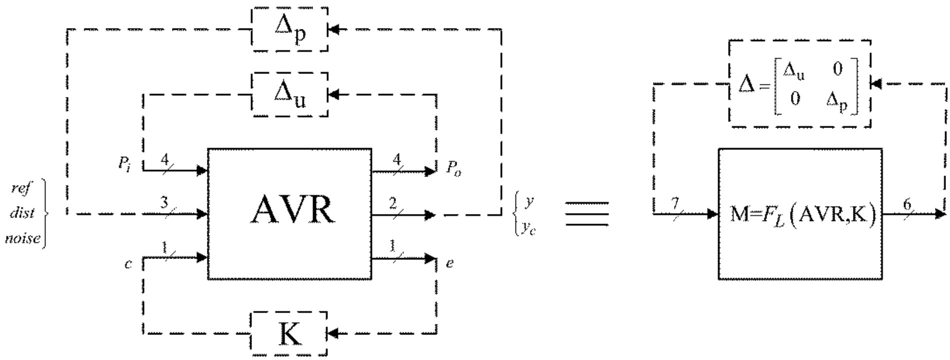

Figure 11. Standard arrangement of P-Δ_u-K of AVR system including weighting functions to determine stability and robust performance.

```
systemnames='AVR_Plant  wp wu wdis wnoise wref';
inputvar='[pert{4} ; ref ; dis ; noise ; control]';
outputvar='[AVR_Plant(1:4) ; wp ; wu ; AVR_Plant(6) ]';
input_to_ AVR_Plant ='[pert(1:4);wref;wdis;wnoise;control]';
input_to_wp='[wref- AVR_Plant(5)]';
input_to_wu='[control]';
input_to_wdis='[dis]';
input_to_wnoise='[noise]';
input_to_wref='[ref]';
sysoutname='AVR';
cleanupsysic='yes';
sysic
%%%%%%%%%%%%%%%%%%%%%%%%%%%%%%%%%%%%%%%%%%%%%%%%%%%%%%%%%%%%
```

```
systemnames='AVR  K1';
inputvar='[pert{4} ; ref ; dis ; noise]';
outputvar='[AVR(1:6)]';
input_to_AVR ='[pert ; ref ; dis ; noise ; K1 ]';
input_to_K1='[AVR(7)]';
sysoutname='M';
cleanupsysic='yes';
```

6- Flowchart for checking the robust stability of the AVR system based on μ theorem

Based on previous explanations, the process of determining the P-Δ_u-K model based on the μ theory for the synchronous generator voltage regulation system (AVR) could be structured based on the flowchart in Figure 12. The main steps of this flowchart are:

1- Determining minimum, maximum, and nominal values of system parameters based on equations 1 to 5.
2- Defining the perturbation plant P based on equations 8 to 12 and constructing the AVR_Plant block of Figure 9.
3- Defining the desired weighting functions of figure 10 and constructing the AVR block of Figure 11 by Matlab sysic command.(Note: if the target is robust stabilty, consider the wegiting functions equal 1)
4- Consider your desired controller's transfer function or steady-state equations and calculate the block M of Figure 11 by lower fractional transformation (LFT).
5- Separate the steady-state equations of M_{11} from the M block of Figure 11.
6- Calculate $\mu_{\Delta_u}(M_{11})$ for your desired frequency range and plot its curve. If this curve is under the 1 for all frequency range, the robust stability is guranteed. Otherwise, the controller does not satisfy the robust stability.
7- To study the robust performance, calculate $\mu_{\Delta}(M)$ for your desired frequency range and plot its curve. If this curve is under the 1 for all frequency range, the robust performance is guranteed. Otherwise, the controller does not satisfy the robust performance.

7- Investigating the robust stability of optimized PID controllers for AVR system

In this part, three PID controllers optimized with meta-heuristic algorithms [11],[37, 38], will be checked for the robust stability of the AVR closed loop system. And it will be shown that the design of the controller at the selected

operating point of these references, will not be able to ensure the stability of the AVR system in the entire range of parameter changes and uncertainties. This will be shown both through the μ curve and through time domain simulation at the maximum, minimum, and nominal points of the system parameters. Table 2 shows the values of the coefficients of the PID controllers of these three references. These coefficients have been obtained through different meta-heuristic optimization and the minimization of different cost functions. However, the design has been done in all three references for the same values of AVR system parameters. These nominal parameters are:

$$\left(K_a=10\ ,\ T_a=0.1\text{s}\ ,\ K_e=1\ ,\ T_e=0.4\ \text{s}\ ,K_g=1\ ,\ T_g=1\text{s}\ ,\ K_s=1\ ,\ T_s=0.01\text{s}\right)$$

Table 2. PID controller coefficients designed for synchronous generator voltage regulation system (AVR) in references [11],[37, 38]

References	K_p	K_i	K_d	T	conversion function
[11]	0.530 2	0.400 1	0.178 7	0.000 1	$K=K_p+\frac{K_i}{s}+\frac{K_d s}{T s+1}$
[37]	0.626 5	0.404 5	0.248 0	0.000 1	$K=K_p+\frac{K_i}{s}+\frac{K_d s}{T s+1}$
[38]	1.128 1	0.956 7	0.567 1	0.000 1	$K=K_p+\frac{K_i}{s}+\frac{K_d s}{T s+1}$

Note that there is no need to introduce weighting functions to check the robust stability and the solution can only be reached through the structure of Figure 9 by checking the $\mu_{\Delta_u}(M_{11})<1$ condition. The $\mu_{\Delta_u}(M_{11})$ value of the P-Δ_u-K model for the real structured uncertainty block $\left(\Delta_u=diag\left(\delta_{KF},\delta_{TA},\delta_{TE},\delta_{TG}\right)\right)$ and weighting functions equal to one is presented in Figure 13. According to Figure 13, it is obvious that the value of $\mu_{\Delta_u}(M_{11})$ in the frequency range of 10 to 100 rad/s is greater than one. Therefore, none of the introduced controllers can provide the robust stability of the closed-loop AVR system in the entire range of system parameter changes.

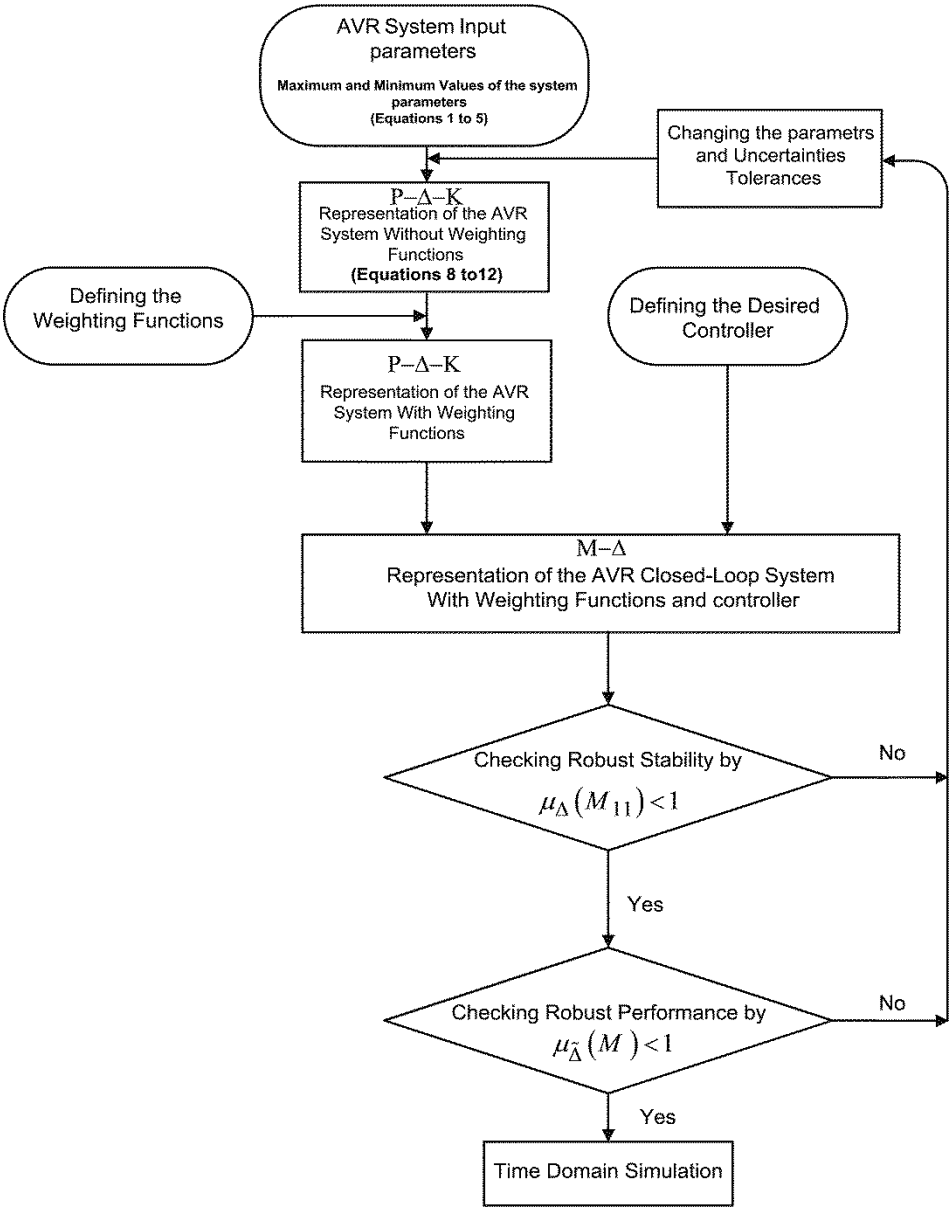

Figure 12. The flow chart of the robust control strategy presented for the automatic regulator of the terminal voltage of the synchronous generator (AVR).

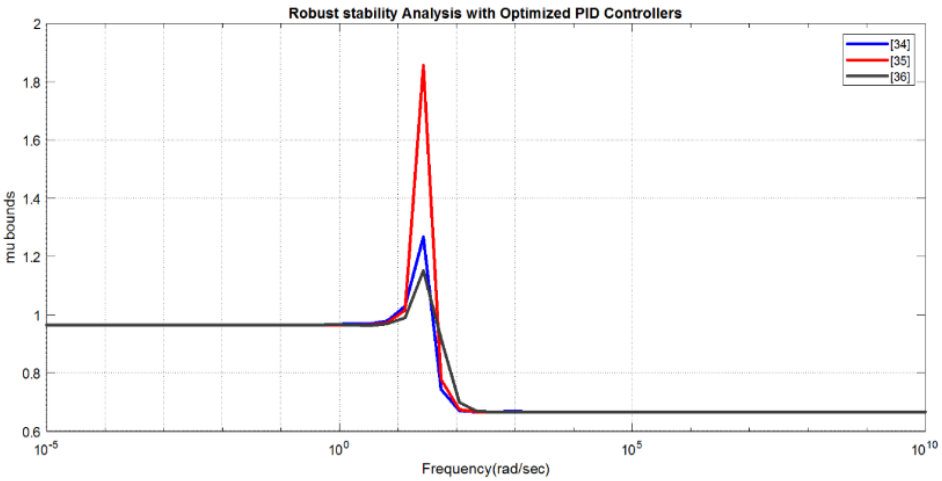

Figure 13. Robust stability curve for PID controllers of references [11],[37, 38]

8- Simulation of optimized PID controllers for AVR system in the time domain

To simulate the time domain, the structure of Figure 3 has been used without considering the disturbance and noise inputs. The goal in this simulation is the sequence on the terminal voltage output of the generator from the input of the base 1 priunit. Simulations have been performed at 5 functional points. These points have been selected considering the system parameters in maximum, minimum and nominal values (average of maximum and minimum points). Figures 14, 15 and 16 show the results of time domain simulation for PID controllers of references [11],[37, 38] respectively.

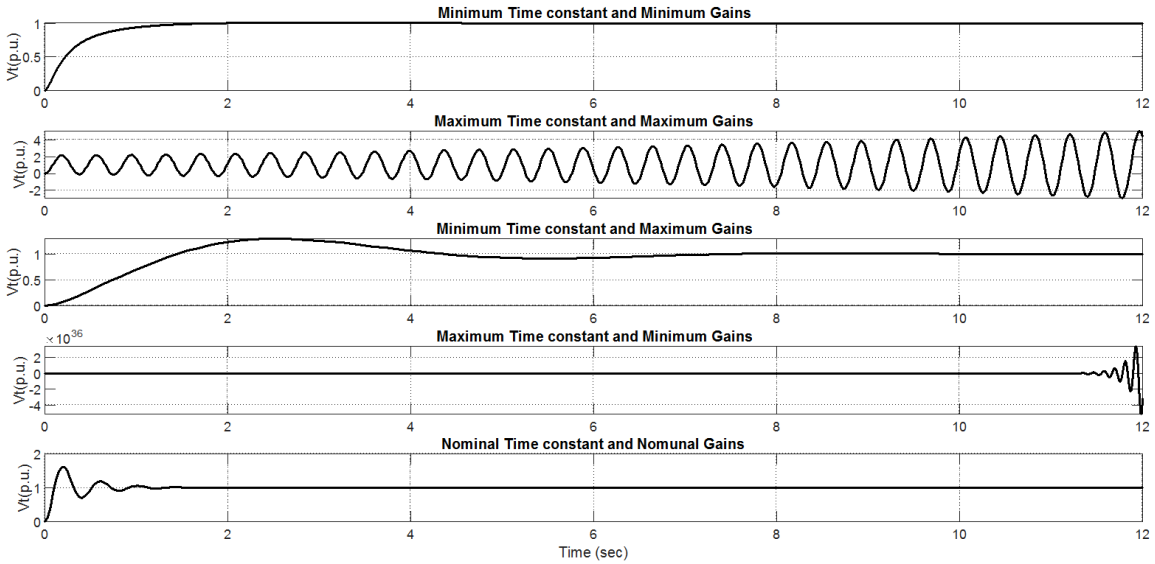

Figure 14. Simulation related to the sequence error of the AVR system from the base input for the reference PID controller [11].

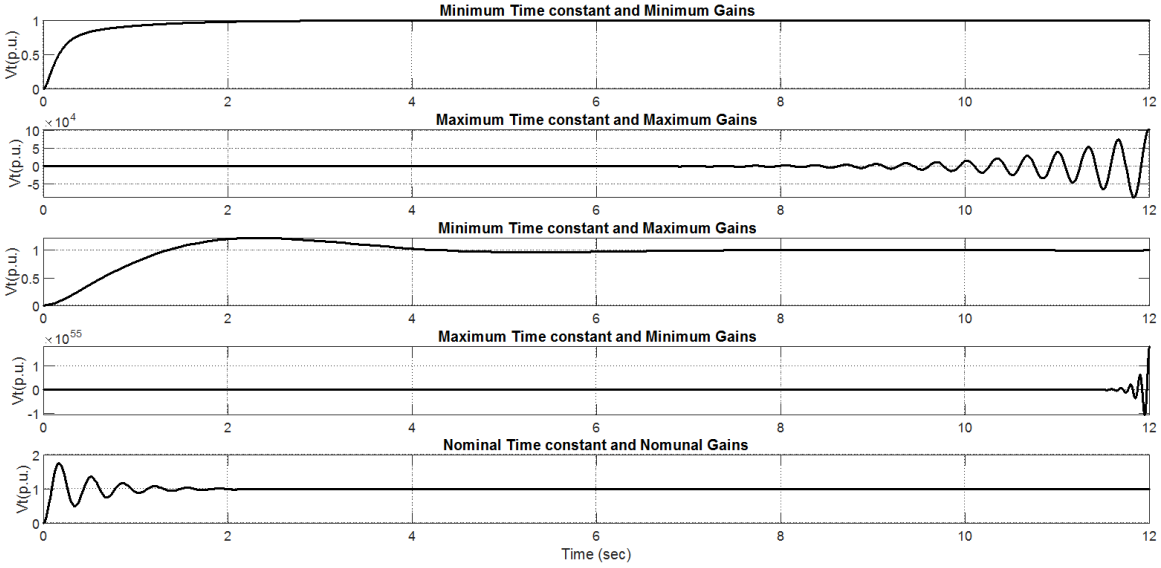

Figure 15. Simulation related to the sequence error of the AVR system from the base input for the reference PID controller [37].

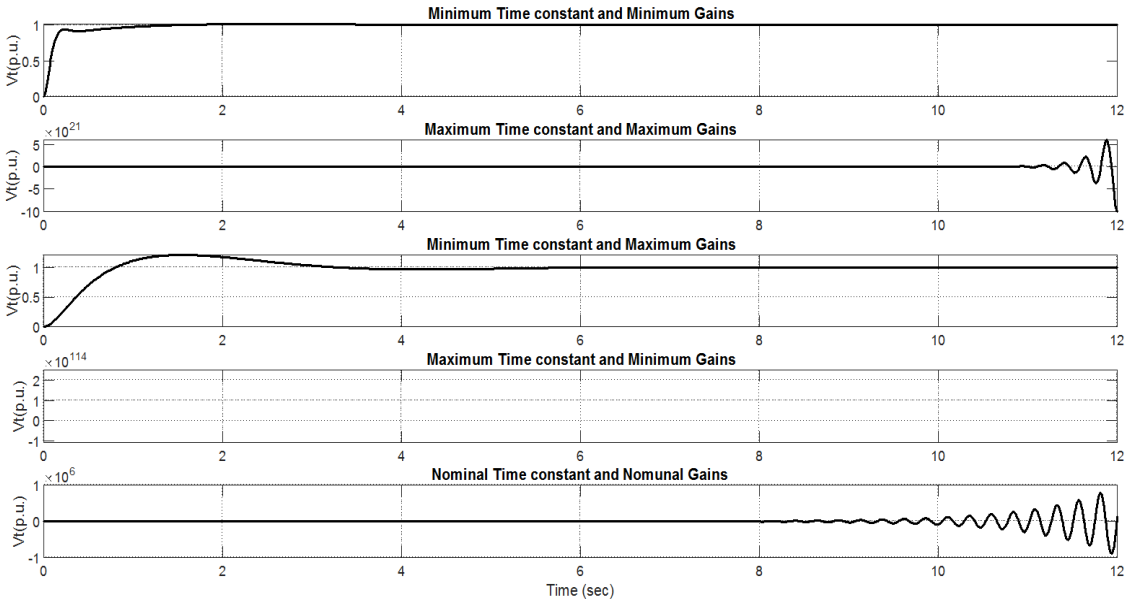

Figure 16. Simulation related to the sequence error of the AVR system from the base input for the reference PID controller [38].

According to these simulations, it is clear that when the gain values or the time constants of the system conversion functions increase, none of the controllers are able to provide the stability of the closed loop structure [11],[37, 38].

9- Conclusion

This paper presents a P-K model for the AVR system based on the model's real parameters and uncertainties with the use of the robust control-related foundations, Mu theorem, and H-inf approach. This model can be easily used to mathematically prove the robust stability of any linear controller designed for the AVR system. A generalized version of this model is also presented in the presence of weighting functions defined to consider robust performance concepts so that it is possible to analyze and design robust controllers for the AVR system. Also, to facilitate the application and generalizability of the subject, the Matlab program used to define the P-K model of the AVR system is presented. Finally, the Mu curve and Matlab simulations associated with three AVR's PID controllers optimized with metaheuristic algorithms are examined to evaluate the presented method.

References

[1]DeMello, F., *Concepts of synchronous machine stability as affected by excitation control.* IEEE Trans. Power Apparatus Syst., 1968. **88**: 180.

[2]Ang, K.H., G. Chong, and Y. Li, *PID control system analysis, design, and technology.* IEEE transactions on control systems technology, 2005. **13**(4): 559-576. doi.org/10.1109/TCST.2005.847331

[3]Modabbernia, M., et al., *Designing the robust fuzzy PI and fuzzy type-2 PI controllers by metaheuristic optimizing algorithms for AVR system.* IETE Journal of Research, 2022. **68**(5): 3540-3554. doi.org/10.1080/03772063.2020.1769510

[4]Gaing, Z.-L., *A particle swarm optimization approach for optimum design of PID controller in AVR system.* IEEE transactions on energy conversion, 2004. **19**(2): 384-391. doi.org/10.1109/TEC.2003.821821

[5]Gozde, H., M.C. Taplamacioglu, and I. Kocaarslan, *Comparative performance analysis of Artificial Bee Colony algorithm in automatic generation control for interconnected reheat thermal power system.* International Journal of Electrical Power & Energy Systems, 2012. **42**(1): 167-178. doi.org/10.1016/j.ijepes.2012.03.039

[6]Gozde, H. and M.C. Taplamacioglu, *Comparative performance analysis of artificial bee colony algorithm for automatic voltage regulator (AVR) system.* Journal of the Franklin Institute, 2011. **348**(8): 1927-1946. doi.org/10.1016/j.jfranklin.2011.05.012

[7]Shirvani, M., et al., *PID power system stabilizer design based on shuffled frog leaping algorithm.* LIFE SCIENCE JOURNAL-ACTA ZHENGZHOU UNIVERSITY OVERSEAS EDITION, 2012. **9**(2): 1065-1070.

[8]Panda, S., B.K. Sahu, and P.K. Mohanty, *Design and performance analysis of PID controller for an automatic voltage regulator system using simplified particle swarm optimization.* Journal of the Franklin Institute, 2012. **349**(8): 2609-2625. doi.org/10.1016/j.jfranklin.2012. 06.008

[9]Hasanien, H.M., *Design optimization of PID controller in automatic voltage regulator system using Taguchi combined genetic algorithm method.* IEEE systems journal, 2012. **7**(4): 825-831. doi.org/ 10.1109/JSYST.2012.2219912

[10]Mohanty, P.K., B.K. Sahu, and S. Panda, *Tuning and assessment of proportional–integral–derivative controller for an automatic voltage regulator system employing local unimodal sampling algorithm.* Electric Power Components and Systems, 2014. **42**(9): 959-969. doi.org/ 10.1080/15325008.2014.903546

[11]Chatterjee, S. and V. Mukherjee, *PID controller for automatic voltage regulator using teaching–learning based optimization technique.* International Journal of Electrical Power & Energy Systems, 2016. **77**: 418-429. doi.org/10.1016/j.ijepes.2015.11.010

[12]Reza Abbasi, B.M., Ali rostamkhani, Hamed Gholizade, *Optimum Design of Automatic Voltage Regulator Based on PID Controller using Imperialistic Competition Algorithm.* Journal of Automotive and Applied Mechanics, 2015. **3**(1).

[13]Devaraj, D. and B. Selvabala, *Real-coded genetic algorithm and fuzzy logic approach for real-time tuning of proportional–integral–derivative controller in automatic voltage regulator system.* IET generation, transmission & distribution, 2009. **3**(7): 641-649. doi.org/10.1049/iet-gtd.2008.0287

[14]Tang, Y., et al., *Optimum design of fractional order PIλDμ controller for AVR system using chaotic ant swarm.* Expert Systems with Applications, 2012. **39**(8): 6887-6896. doi.org/10.1016/j.eswa.2012.01.007

[15]Ramezanian, H., S. Balochian, and A. Zare, *Design of optimal fractional-order PID controllers using particle swarm optimization algorithm for automatic voltage regulator (AVR) system.* Journal of Control, Automation and Electrical Systems, 2013. **24**(5): 601-611. doi.org/ 10.1007/s40313-013-0057-7

[16]Aguila-Camacho, N. and M.A. Duarte-Mermoud, *Fractional adaptive control for an automatic voltage regulator.* ISA transactions, 2013. **52**(6): 807-815. doi.org/10.1016/j.isatra.2013.06.005

[17]Zhang, D.-L., T. Ying-Gan, and G. Xin-Ping, *Optimum design of fractional order PID controller for an AVR system using an improved artificial bee colony algorithm.* Acta Automatica Sinica, 2014. **40**(5): 973-979. doi.org/10.1016/S1874-1029(14)60010-0

[18]Das, S. and I. Pan, *On the Mixed ${{\rm H} _2}/{{\rm H} _\infty} $ Loop-Shaping Tradeoffs in Fractional-Order Control of the AVR System.* IEEE Transactions on Industrial Informatics, 2014. **10**(4): 1982-1991. doi.org/10.1109/TII.2014.2322812

[19]Tang, Y., et al., *Optimal gray PID controller design for automatic voltage regulator system via imperialist competitive algorithm.* International Journal of Machine Learning and Cybernetics, 2016. **7**: 229-240. doi.org/10.1007/s13042-015-0431-9

[20]Mukherjee, V. and S. Ghoshal, *Intelligent particle swarm optimized fuzzy PID controller for AVR system.* Electric Power Systems Research, 2007. **77**(12): 1689-1698. doi.org/10.1016/j.epsr.2006.12.004

[21]Jahedi, G. and M. Ardehali, *Genetic algorithm-based fuzzy-PID control methodologies for enhancement of energy efficiency of a dynamic energy system.* Energy Conversion and Management, 2011. **52**(1): 725-732. doi.org/10.1016/j.enconman.2010.07.051

[22]Shabib, G., *Implementation of a discrete fuzzy PID excitation controller for power system damping.* Ain Shams Engineering Journal, 2012. **3**(2): 123-131. doi.org/10.1016/j.asej.2011.12.001

[23]Panda, M.K., G.N. Pillai, and V. Kumar, *Design of an interval type-2 fuzzy logic controller for automatic voltage regulator system.* Electric Power Components and Systems, 2011. **40**(2): 219-235. doi.org/10. 1080/15325008.2011.629336

[24]Sahib, M.A., *A novel optimal PID plus second order derivative controller for AVR system.* Engineering Science and Technology, an International Journal, 2015. **18**(2): 194-206. doi.org/10.1016/j.jestch.2014.11.006

[25]Sikander, A., et al., *A novel technique to design cuckoo search based FOPID controller for AVR in power systems.* Computers & Electrical Engineering, 2018. **70**: 261-274. doi.org/10.1016/j.compeleceng.2017 .07.005

[26]Micev, M., M. Ćalasan, and D. Oliva, *Design and robustness analysis of an Automatic Voltage Regulator system controller by using Equilibrium Optimizer algorithm.* Computers & Electrical Engineering, 2021. **89**: 106930. doi.org/10.1016/j.compeleceng.2020.106930

[27]Modabbernia, M., et al., *Robust control of automatic voltage regulator (AVR) with real structured parametric uncertainties based on H∞ and μ-analysis.* ISA transactions, 2020. **100**: 46-62. doi.org/10.1016/j.isatra. 2020.01.010

[28]Fan, L. *Review of robust feedback control applications in power systems*. in *2009 IEEE/PES Power Systems Conference and Exposition*. 2009. IEEE. doi.org/10.1109/PSCE.2009.4840041

[29]Qihua and J. Jiang, *Robust controller design for generator excitation systems.* IEEE Transactions on Energy Conversion, 1995. **10**(2): 201-209. doi.org/10.1109/60.391883

[30]Bouhamida, M., A. Mokhtari, and M. Denai, *Power system stabilizer design based on robust control techniques.* ACSE journal, 2005. **5**(3).

[31]Mirzaei, M., H.H. Niemann, and N.K. Poulsen. *DK-iteration robust control design of a wind turbine*. in *2011 IEEE International Conference on Control Applications (CCA)*. 2011. IEEE. doi.org/10.1109/ CCA.2011.6044429

[32]Chen, S. and O. Malik, *Power system stabilizer design using/spl mu/synthesis.* IEEE Transactions on Energy Conversion, 1995. **10**(1): 175-181. doi.org/10.1109/60.372584

[33]H., S., *Power System Analysis*. Third ed. 2011: PSA Publishing LLC.

[34]Gu, D.-W., P. Petkov, and M.M. Konstantinov, *Robust control design with MATLAB®*. 2005: Springer Science & Business Media.

[35]Khalil, I., J. Doyle, and K. Glover, *Robust and optimal control*. 2. 1996: Prentice Hall New York.

[36]Modabbernia, M., et al., *A novel robust strategy for the concurrent control of frequency and voltage in the synchronous generator with real structured uncertainties.* Electric Power Components and Systems, 2022. **50**(16-17): 1029-1050. doi.org/10.1080/15325008.2022.2145388

[37]Pazhanimuthu, C., et al., *Performance analysis of voltage profile improvement in AVR system using zebra optimization algorithms based on PID controller.* e-Prime-

Advances in Electrical Engineering, Electronics and Energy, 2023. **6**: 100380. doi.org/10.1016/j.prime. 2023.100380

[38]Köse, E., *Optimal control of AVR system with tree seed algorithm-based PID controller.* IEEE access, 2020. **8**: 89457-89467. doi.org/10.1109/ ACCESS.2020.2993628